Impacts of Hypoxia-Inducible Factor-1 Knockout in the Retinal Pigment Epithelium on Choroidal Neovascularization

Mingkai Lin,[1–3] *Yang Hu,*[1] *Ying Chen,*[1] *Kevin K. Zhou,*[1] *Ji Jin,*[1] *Meili Zhu,*[4,6] *Yun-Zheng Le,*[4–6] *Jian Ge,*[2,3] *and Jian-xing Ma*[1,4,6]

Purpose. Hypoxia-inducible factor (HIF)-1 is a key oxygen sensor and is believed to play an important role in neovascularization (NV). The purpose of this study is to determine the role of retinal pigment epithelium (RPE)-derived HIF-1α on ocular NV.

Methods. Conditional *HIF-1α* knockout (KO) mice were generated by crossing transgenic mice expressing *Cre* in the RPE with *HIF-1α* floxed mice, confirmed by immunohistochemistry, Western blot analysis, and fundus fluorescein angiography. The mice were used for the oxygen-induced retinopathy (OIR) and laser-induced choroidal neovascularization (CNV) models.

Results. HIF-1α levels were significantly decreased in the RPE layer of ocular sections and in primary RPE cells from the *HIF-1α* KO mice. Under normal conditions, the *HIF-1α* KO mice exhibited no apparent abnormalities in retinal histology or visual function as shown by light microscopy and electroretinogram recording, respectively. The *HIF-1α* KO mice with OIR showed no significant difference from the wild-type (WT) mice in retinal levels of HIF-1α and VEGF as well as in the number of preretinal neovascular cells. In the laser-induced CNV model, however, the disruption of *HIF-1α* in the RPE attenuated the over expression of VEGF and the intercellular adhesion molecule 1 (ICAM-1), and reduced vascular leakage and CNV area.

Conclusions. RPE-derived HIF-1α plays a key role in CNV, but not in ischemia-induced retinal NV. (*Invest Ophthalmol Vis Sci.* 2012;53:6197–6206) DOI:10.1167/iovs.11-8936

Ocular neovascularization (NV) and retinal vascular leakage are common causes of vision loss. Retinal NV refers to abnormal growth of retinal blood vessels that usually break through the inner limiting membrane and grow into the vitreous. Retinal NV often occurs in diabetic retinopathy and retinopathy of prematurity.[1,2] Choroidal neovascularization (CNV) refers to NV that originates from choroidal vessels that penetrate Bruch's membrane and invade the subretinal space. CNV is a characteristic pathologic change in the wet form of AMD.[3] Although the anti-VEGF compounds are effective in most CNV cases, the pathogenesis of ocular NV is not completely understood, and long-term treatments are required for CNV.

VEGF is known to be a key stimulator of ocular NV.[4] Hypoxia is believed to be a major inducer of VEGF overexpression in retinal NV and CNV.[5] Hypoxia can occur secondary to many diseases[6] and induces multiple pro-angiogenic cytokines, including VEGF, through hypoxia-inducible factors (HIF).[7] Extensive studies have shown that HIF-1 is a key oxygen sensor and mediator of angiogenesis.[8–10] HIF-1 is a heterodimer consisting of an inducible HIF-1α subunit and a constitutively-expressed HIF-1β subunit[11] In the presence of oxygen, HIF-1α is constantly expressed and rapidly degraded after its binding to the von Hippel-Lindau tumor-suppressor protein (VHL). VHL binding is dependent on the hydroxylation of Pro-402, Pro-564, or both by prolyl hydroxylase domain protein 2 (PHD_2).[12,13] Under hypoxic conditions, PHD_2 activity decreases,[14,15] and consequently, HIF-1α is stabilized and accumulates. It then dimerizes with HIF-1β and translocates into the nucleus, activating the transcription of target genes such as VEGF and erythropoietin (EPO), which are important pathogenic factors in NV.[16]

The retinal pigment epithelium (RPE) is located between the neural retina and the vascular choriocapillaris. The RPE forms the outer blood–retina barrier (BRB) and serves as the gatekeeper for the neural retina, controlling the passage of metabolites to and from the circulatory system, renewing photoreceptor outer segment discs and providing 11-cis-retinal for phototransduction.[17] Experimental and clinical evidence have demonstrated that altered gene expression in the RPE contributes to some retinal and choroidal diseases.[18] It has been shown that HIF-1 and VEGF are expressed in all of the cell types of the retina.[19] RPE-derived VEGF has been shown to play an important role in maintaining the physiological fenestration of choroidal vessels.[20] Disruption of RPE-derived VEGF at embryonic day 10 (E10) prevents the development of choriocapillaris, promotes microphthalmia, and results in complete loss of visual function.[21] The disruption of RPE-derived VEGF after E15 using conditional VEGF knockout (KO) mice with an inducible Cre/lox system did not cause detectable developmental defects.[22]

VEGF is known to be regulated by multiple transcription factors and pathways.[23] To determine the role of RPE-derived HIF-1 in ischemia-induced VEGF over production and ocular NV, we knocked out HIF-1α in the RPE using the Cre/lox

From the Departments of [1]Physiology, [4]Medicine, and [5]Cell Biology, and the [6]Harold Hamm Diabetes Center, The University of Oklahoma Health Sciences Center, Oklahoma City, Oklahoma; and the [2]State Key Laboratory of Ophthalmology and the [3]Zhongshan Ophthalmic Center, Sun Yat-sen University, Guangzhou, China.

Supported by grants from the National Institute of Health (EY018659, EY019309, EY012231, EY20900, P20RR024215), from the American Diabetes Association (ADA), Foundation Fighting Blindness (FFB), grants from Guangdong Provincial Department of Science and Technology (2011B031800176), and the Zhongshan Ophthalmic Center (3030901010037).

Submitted for publication October 28, 2011; revised April 6 and July 29, 2012; accepted August 12, 2012.

Disclosure: **M. Lin**, None; **Y. Hu**, None; **Y. Chen**, None; **K.K. Zhou**, None; **J. Jin**, None; **M. Zhu**, None; **Y.-Z. Le**, None; **J. Ge**, None; **J. Ma**, None

Corresponding author: Jian-xing Ma, 941 Stanton L. Young Boulevard, BSEB 328B, Oklahoma City, OK 73104; jian-xing-ma@ouhsc.edu.

system. This report describes our initial characterization of the conditional *HIF-1α* KO mice in ischemia-induced retinal NV and laser-induced CNV.

Methods

Generation of Conditional HIF-1α KO Mice and Animal Treatment

All animal experiments were performed following the guidelines of the ARVO statement for the Use of Animals in Ophthalmic and Vision Research and approved by the Institutional Animal Care and Use Committee. The conditional *HIF-1α* KO mice were generated by crossing transgenic mice expressing Cre in the RPE with *HIF-1α*–floxed mice (See Supplementary Material and Supplementary Fig. S1A, http://www.iovs.org/lookup/suppl/doi:10.1167/iovs.11-8936/-/DCSupplemental)[21] Primer sequences for genotyping were as follows: Primers a (5′-GCAGTTAAGAGCAC TAGTTG-3′) and b (5′-GGAGCTATCTCCTAGACC-3′) were used for genomic PCR to detect a 280-bp product for the floxed *HIF-1α* allele, and a 220-bp product for the WT allele (See Supplementary Material and Supplementary Fig. S1B, http://www.iovs.org/lookup/suppl/doi:10.1167/iovs.11-8936/-/DCSupplemental)[19]; primers c (5′-AGGTGTAGAGAAGGCACTTAGC-3′) and d (5′-CTAATCGCCATCTTC CAGCAGG-3′) were used to amplify a 411-bp product for Cre (See Supplementary Material and Supplementary Fig. S1B, http://www.iovs.org/lookup/suppl/doi:10.1167/iovs.11-8936/-/DCSupplemental).[24] Disruption of *HIF-1α* was enhanced by feeding the mice doxycycline at a dose of 2 mg/mL in 5% sucrose solution from E15 to postnatal day 1 (P1).

Oxygen-induced retinopathy (OIR) was generated by exposing mice to 75% oxygen in a chamber from P7 to P12 and then returning them to room air at P12.

Laser-induced CNV was generated following a documented protocol.[25] Briefly, 2-month-old mice were anesthetized with an intraperitoneal injection of ketamine (100 mg/kg) and xylazine (10 mg/kg). The pupils were then dilated with 1% tropicamide. For generating laser burns, the Solitaire Photocoagulaor (REF: LP 4532; Ellex Medical Pty Ltd, Adelaide SA 5000, Australia) was used with a double aspheric 28 diopter (D)-lens (Volk, Mentor, OH) under a fixed indirect ophthalmoscope. Four 532-nm diode laser spots (160 mw, 100 msec) were applied to each fundus between retinal vessels 2 to 3 disc diameters from the optic nerve (See Supplementary Material and Supplementary Figs. S2A, S2B, http://www.iovs.org/lookup/suppl/doi:10.1167/iovs.11-8936/-/DCSupplemental). Only the eyes with bubble formation at the time of laser application, which indicates rupture of Bruch's membrane (See Supplementary Material and Supplementary Figs. S2C, S2D, http://www.iovs.org/lookup/suppl/doi:10.1167/iovs.11-8936/-/DCSupplemental), were included in the study. Fundus pictures were taken with a Kowa Genesis-D Hand-held Retinal Camera (Kowa Company Ltd, Tokyo, Japan).

Primary RPE Cell Culture

Primary RPE cells were isolated and cultured as described previously.[26] The eyes from 14-day-old pups were washed twice in Dulbecco's modified eagle's medium (DMEM) (Mediatech, Inc., Manassas, VA), and incubated in 2% Dispase in DMEM for 45 minutes at 37°C. The enzyme solution was removed and enzymatic activity quickly quenched with DMEM supplemented with 10% fetal bovine serum (FBS), 1% penicillin/streptomycin, 2.5 mM L-glutamine, and 1% nonessential amino acids. After removal of the cornea, iris, and lens, the posterior eyecup was placed in fresh growth medium and incubated for 20 minutes at 37°C in 5% CO_2. The neural retina and the RPE sheet were separately peeled from the eyecup using fine forceps. The RPE sheets were resuspended in 0.05% trypsin solution for no more than 5 minutes to disperse the cells into a single cell suspension. Cultured cells from passages four to six were used, and the cells were exposed to serum-free DMEM before analysis.

Electroretinogram (ERG) Recording

ERG measurement was performed as described previously.[27] ERG was recorded with a gold electrode placed on the cornea, a reference electrode in the mouth, and a ground electrode on the tail. Dark adaptation was for 12 hours and the light adaption was for 15 minutes. The flash intensities for scotopic and photopic ERG were 1000 and 2000 cd.s/m^2, respectively. The ERG waveforms of both eyes in the same animal were simultaneously recorded. The b-wave amplitude was measured between the peaks of the a- and b-waves.

Retinal Morphology Examination

Eyes were fixed in Perfix solution (4% paraformaldehyde, 20% isopropanol, 2% trichloroacetic acid, and 2% zinc chloride) for 48 hours, embedded in paraffin, and sectioned (5-μm thickness). Sections were stained with haematoxylin and eosin (H&E) and examined under a light microscope. Morphometric analysis of retinal sections was performed as described previously.[28]

Western Blot Analysis

Western blot analysis was performed as described previously.[29,30] For in vitro assays, cell lysates were prepared from primary RPE cells exposed to normoxia or hypoxia (1% oxygen) for 12 hours. For in vivo assays, mice were anesthetized and perfused with PBS. Both of the retinae (in 200 μL) or the RPE/choroid complexes (in 150 μL) from each mouse, from one eyecup (in 150 μL) was dissected and homogenized in ice-cold tissue lysis buffer (50 mmol/L Tris-HCl, pH 7.4, 2 mmol/L $MgCl_2$, 1% NP-40, 10% glycerol, and 100 mmol/L NaCl) and a protease inhibitor cocktail (1:100 dilution; Sigma Aldrich, St. Louis, MO) was added. Bradford assay was used to determine the protein concentration. Rabbit anti–HIF-1α antibody (1:2000 dilution; Novus Biologicals NB100-479, Littleton, CO), rabbit anti-VEGF antibody (A20, 1:500 dilution; Santa Cruz Biotechnologies, Santa Cruz, CA), mouse anti–β-actin antibody (1:4000 dilution; Abcam, Cambridge, MA), mouse anti-VEGF antibody (C1, 1:500 dilution; Santa Cruz Biotechnologies), goat anti-albumin antibody (1:3000 dilution; Bethyl Laboratories, Montgomery, TX), and goat anti-intercellular adhesion molecule 1 (ICAM-1) antibody (1:500 dilution; Santa Cruz Biotechnologies) were used to detect each protein and blotted with a horseradish peroxidase-conjugated secondary antibody. The signal was developed with Super Signal West Dura Extended Duration Substrate (Thermo Scientific, Rockford, IL), and images were captured by a Chemi Genius Image Station (SynGene, Frederick, MD). Densitometry was used for semiquantification of each protein level with the GENETOOLS program (SynGene) via normalization to β-actin levels.

Quantitative Real-Time RT–PCR

Total RNA was isolated from the eyecup using Trizol according to the manufacturer's protocol (Invitrogen, Carlsbad, CA). mRNAs were reverse-transcribed and amplified by quantitative PCR as described previously.[29] Real-time RT-PCR was performed using primers 5′-GCA TTT CTG GGG ATT GCT TA-3′ and 5′- ATT CTC CCA CCG TCA GTA CG –3′ for *Cre*, 5′-TCA AGT CAG CAA CGT GGA AG-3′ and 5′-TAT CGA GGC TGT GTC GAC TG-3′ for mouse *HIF-1α*, and 5′-TTT GTT GGT TTT CGG AAC TGA-3′ and 5′-CGT TTA TGG TCG GAA CTA CGA-3′ for mouse 18S RNA.

Immunohistochemistry

For in vivo assays, mice were anesthetized and perfused with PBS. The eyes were isolated and incubated for 10 minutes in 4% paraformalde-

hyde in PBS. After the cornea and lens were removed, the posterior eyecups were incubated for another 15 minutes in 4% paraformaldehyde. The eyecups were treated with 10%, 20%, and 30% sucrose, then embedded in Tissue-Tek O.C.T. Compound (Sakura Finetek USA, Torrance, CA). Sections were cut and blocked with a mixture of 10% normal goat serum, 3% bovine serum albumin, and 0.25% Triton X-100. Slides were incubated with the anti–HIF-1α antibody (NB 100–479, 1:100 dilution; Novus Biologicals), mouse anti-VEGF antibody (C1, 1:100 dilution; Santa Cruz Biotechnologies). Nonspecific mouse immunoglobulin G (IgG, 1:100 dilution; Innovative Research, Novi, MI) was used as negative control. The slides were then incubated with Cy3- or FITC-labeled secondary antibodies (Jackson ImmunoResearch Europe, Newmarket, UK) for 1 hour, and mounted with Mounting Medium for Fluorescence with 4′,6-diamidino-2-phenylindole (DAPI) (Vector Laboratories, Burlingame, CA).

For in vitro assays, the cells were fixed with 4% paraformaldehyde for 10 minutes and incubated with 0.1% Triton X-100. The fixed cells were stained with a rabbit anti-retinol dehydrogenases 10 (RDH_{10}) antibody[31] (1:50) or a rabbit anti–HIF-1α antibody (NB 100–479, 1: 1000 dilution; Novus Biologicals). A negative control section was processed similarly, except the primary antibody was omitted.

Retinal Angiography

Fundus fluorescein angiography of CNV lesions was conducted using a Kowa Genesis-D Hand-held Retinal Camera (Kowa Company Ltd). Fundus angiograms were obtained at different time points after an intraperitoneal fluorescein injection (200 mg/kg body weight of 25% fluorescein; Hub Pharmaceuticals, Rancho Cucamonga, CA).

Retinal angiography was performed as described previously.[32] Mice were anesthetized and perfused through the left ventricle with 50 mg/mL high molecular weight fluorescein–dextran (Sigma Aldrich) in PBS. The eyes were enucleated and fixed in 4% paraformaldehyde for 24 hours. After removal of the anterior section, the retina or the RPE/choroid complex was flat-mounted. For analysis of retinal vessel density, angiographic images were used to count the mean of microvessel intersections.[33] For comparison of the CNV lesion, the area of CNV was measured with the SPOT software (SPOT Imaging Solutions, Inc., Sterling Heights, MI).

Quantification of Retinal NV

Preretinal NV was quantified as described previously.[34] Briefly, serial ocular sections (5 μm) from OIR mice were cut sagittally and stained with H&E. Eight discontinuous sections per eye were used to count preretinal vascular cells, which are found on the vitreal side of the inner limiting membrane, since few nuclei can be found in the vitreous in an eye cross-section under normal conditions.

Statistical Analysis

The quantitative data was analyzed and compared with the WT mice using Mann-Whitney *U* test. Statistical significance was set at $P < 0.05$.

Results

Lack of HIF-1α Expression in Primary RPE Cells from Conditional HIF-1α KO Mice

The efficiency of *HIF-1α* disruption was determined using primary RPE cells isolated from the *HIF-1α* KO ($Cre^{+}/HIF\text{-}1\alpha^{ff}$) mice. Primary mouse RPE cells grew as an irregularly shaped monolayer with areas of dense pigmentation (Fig. 1A). The identity of the primary cells was confirmed by immunocytochemistry using an antibody specific for RDH_{10}, a RPE cell marker. The results showed that the isolated cells were RDH_{10}-positive RPE cells (Figs. 1B, 1C). Immunostaining detected HIF-1α signal in the cytoplasm of cells from WT mice ($Cre^{-}/HIF\text{-}1\alpha^{ff}$) exposed to normoxic conditions; under hypoxia, HIF-1α signal was increased in the nuclei, suggesting nuclear translocation (Figs. 1E, 1G, 1I, 1K). Using the same staining conditions as that for the WT cells, RPE cells from the *HIF-1α* KO mice showed only background levels of HIF-1α signal under both normoxic and hypoxic conditions (Figs. 1F, 1H, 1J, 1L).

Western blot analysis demonstrated that in primary RPE cells, total HIF-1α levels from WT controls were approximately 2-fold higher than those from the *HIF-1α* KO mice under normoxia (Figs. 1M, 1N). Under hypoxic conditions, up-regulation of HIF-1α was detected in the WT RPE cells ($P < 0.01$; Figs. 1M, 1N). In contrast, the hypoxia-induced accumulation of HIF-1α was partially attenuated in the RPE cells from *HIF-1α* KO mice (Figs. 1M, 1N).

Expression of *VEGF*, a target gene of HIF-1α, was up-regulated by hypoxia in the WT RPE cells. In contrast, the hypoxia-induced overexpression of *VEGF* was significantly diminished in RPE cells from the *HIF-1α* KO mice. Under normoxic culture conditions, no significant difference was found in *VEGF* expression between the WT and the *HIF-1α* KO cells (Figs. 1M, 1O).

The efficiency of *HIF-1α* disruption was also confirmed by immunohistochemistry of ocular sections and immunoblotting. Immunostaining showed a markedly decreased intensity of HIF-1α signals in the RPE layer of the conditional *HIF-1α* KO mice, compared with that in the age-matched WT mice (Figs. 2A–F; See Supplementary Material and Supplementary Figs. S3A–G, http://www.iovs.org/lookup/suppl/doi:10.1167/iovs.11-8936/-/DCSupplemental). In contrast, the intensity of HIF-1α signals in the neural retina of the *HIF-1α* KO mice was similar to that in the WT mice. Consistently, real-time RT-PCR confirmed that HIF-1α mRNA levels were significantly lower in the eyecups of *HIF-1α* KO mice, compared with that in WT mice (Fig. 2G).

Retinal Development in the Conditional HIF-1α KO Mice

To verify whether the disruption of *HIF-1α* in the RPE affects retinal development, retinal histology, vasculature, and visual function, these phenotypes were carefully analyzed in the conditional *HIF-1α* KO mice. Under normal conditions, no apparent morphological changes in the thickness of the outer nuclear layer (ONL), the inner nuclear layer (INL), and the whole retina was observed in 2-month-old *HIF-1α* KO mice, compared with their WT controls (See Supplementary Material and Supplementary Figs. S3A–C, http://www.iovs.org/lookup/suppl/doi:10.1167/iovs.11-8936/-/DCSupplemental). Fluorescein angiography also demonstrated no significant difference in retinal vascular densities and patterns between WT and *HIF-1α* KO mice at P17 (See Supplemental Material and Supplemental Figs. S3D–F, http://www.iovs.org/lookup/suppl/doi:10.1167/iovs.11-8936/-/DCSupplemental). Furthermore, scotopic and photopic ERG showed no significant difference in amplitudes of a- and b-waves between WT and the *HIF-1α* KO mice at the age of 3 months (See Supplementary Material and Supplementary Figs. S3G, S3H, http://www.iovs.org/lookup/suppl/doi:10.1167/iovs.11-8936/-/DCSupplemental). These results suggest that disruption of *HIF-1α* in the RPE does not impair retinal development or visual function under normal conditions.

Ischemia-Induced Retinopathy in the Conditional HIF-1α KO Mice

The RPE is known as a major source of retinal VEGF under ischemia conditions.[4,35] To determine whether RPE-specific KO of *HIF-1α* affects ischemia-induced retinal NV, the *HIF-1α*

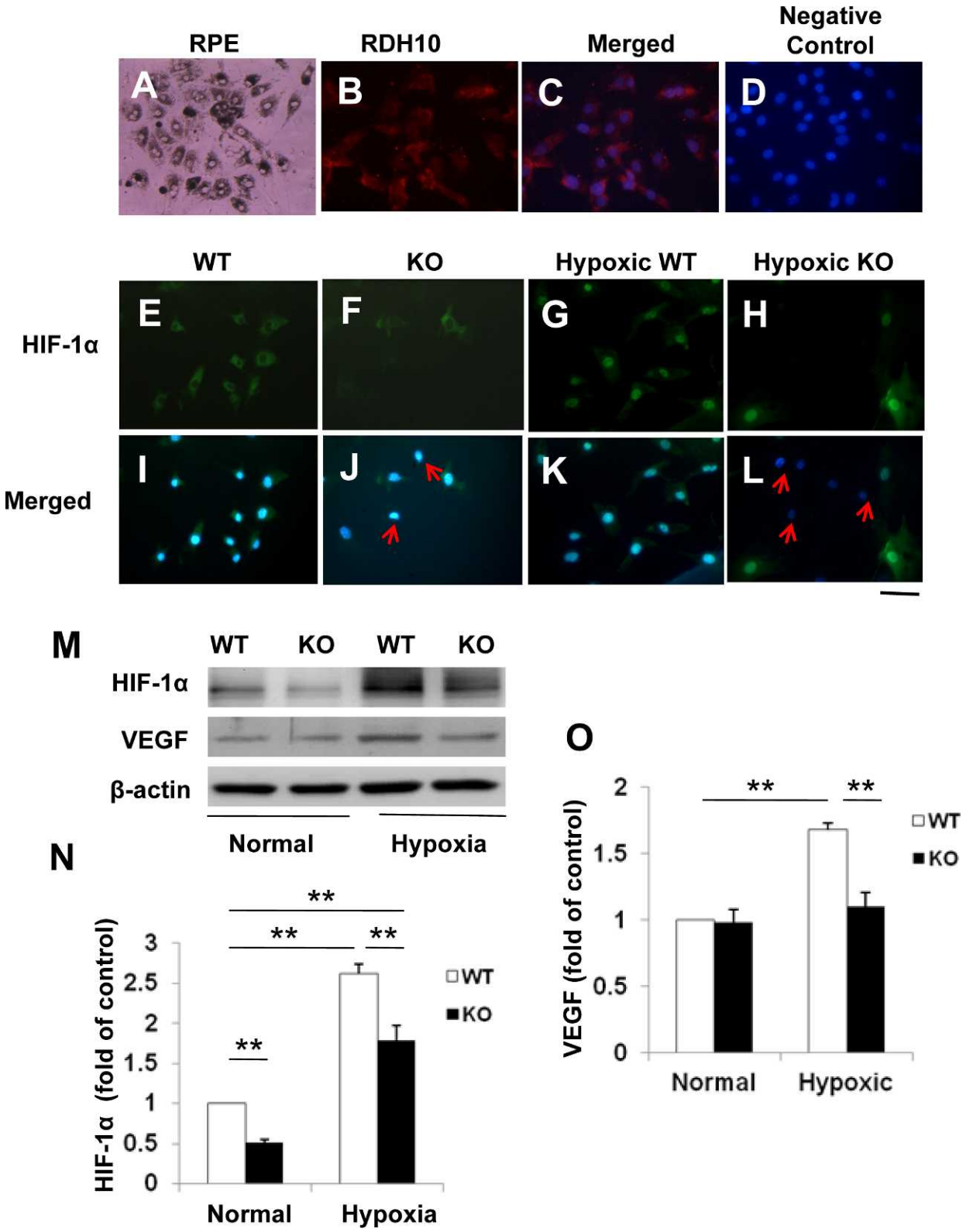

Figure 1. Expression of HIF-1α and VEGF in primary RPE cells isolated from the conditional *HIF-1α* KO mice. (**A**) Light microscope image of primary mouse RPE cells showing areas of dense pigmentation. (**B, C**) The RPE cells were immunostained with an antibody for RDH_{10} (*red*) (**B**), and counterstained with DAPI (*blue*) (**C**); (**D**) Negative control with the primary antibody omitted. (**E–L**) Immunostaining of HIF-1α (*red*) in primary RPE cells from WT and *HIF-1α* KO mice and cultured under normoxic (**E, F, I, J**) or hypoxic (1% oxygen) (**G, H, K, L**) conditions (**E–H**) and counterstained with DAPI (*blue*, **I–L**). Arrows indicate RPE cells with disrupted *HIF-1α*. *Scale bar*, 50 μm. (**M**) Western blot analysis of HIF-1α and VEGF in primary RPE cells. (**N**) HIF-1α levels were significantly decreased in the RPE cells from *HIF-1α* KO mice, compared with that of WT mice under normoxic conditions, as quantified by densitometry and normalized by β-actin levels (not mentioned in the following quantifications). Under hypoxic conditions, HIF-1α levels in the *HIF-1α* KO RPE cells were significantly decreased, compared with that in the WT cells (mean ± SEM, $n = 5$). (**O**) Overexpression of VEGF was significantly attenuated in primary RPE cells from the *HIF-1α* KO mice under hypoxic conditions (mean ± SEM, $n = 5$). $^{**}P < 0.01$.

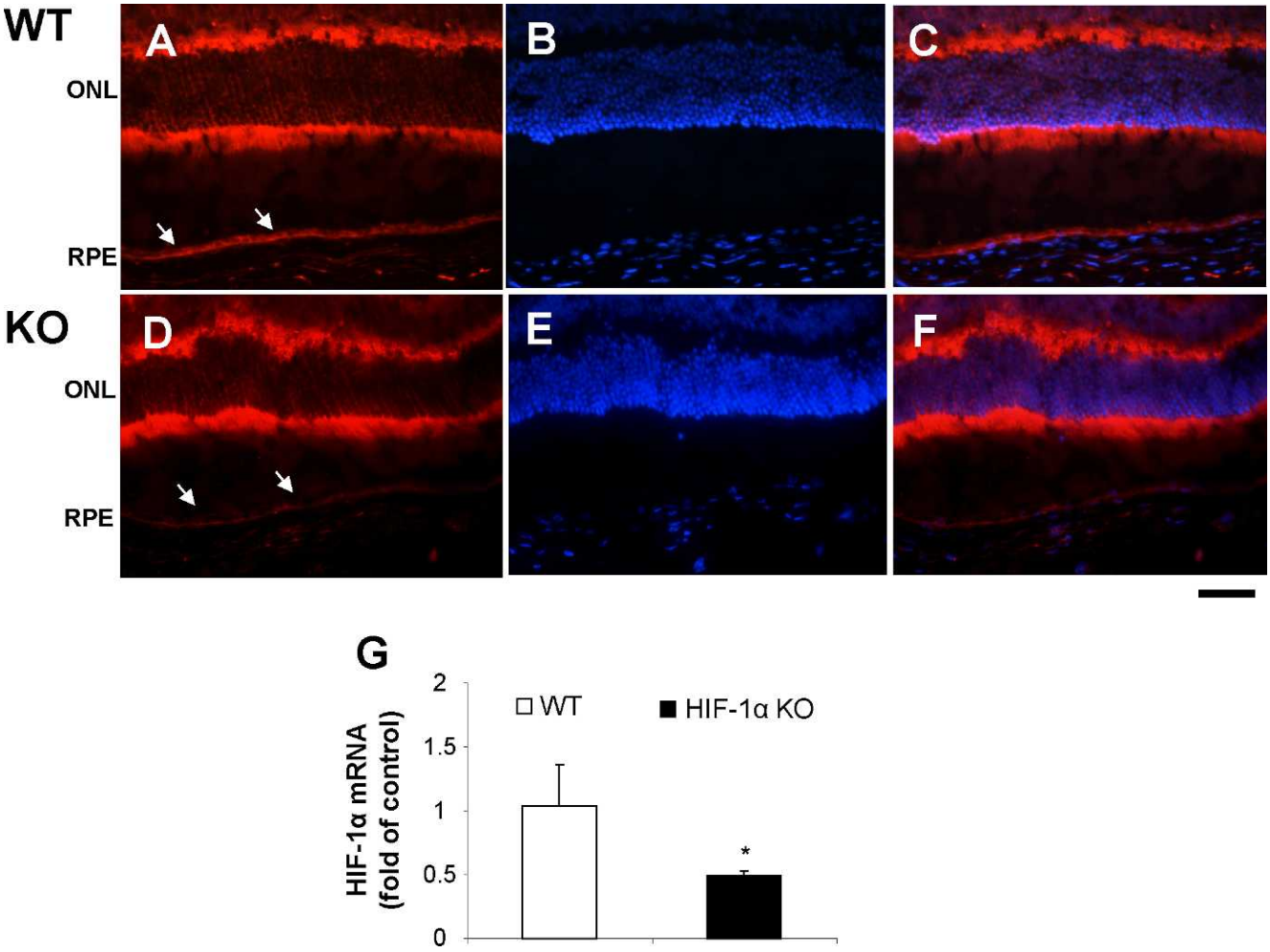

Figure 2. Decreased expression of HIF-1α in the RPE in the *HIF-1α* KO mice**.** Immunostaining of HIF-1α in the retina and RPE from the *HIF-1α* KO and WT control mice under normoxic conditions. *Arrows* indicate the RPE. (**A, D**) HIF-1α staining (*red*); (**B, E**) nuclei stained by DAPI (*blue*); (**C, F**) Merged images. *Scale bar*, 50 μm. (**G**) mRNA alternation of HIF-1α in the eyecups of WT and the *HIF-1α* knockout mice. Real-time RT-PCR analysis of mRNA levels of HIF-1α was performed using RNA from the eyecups of 12-week-old WT mice and age-matched *HIF-1α* KO mice (mean ± SEM, $n = 4$, $^*P < 0.05$).

KO mice were exposed to OIR conditions to induce retinal NV. Under normoxic conditions, no significant differences in retinal levels of HIF-1α and VEGF were detected by Western blot analysis between WT and the *HIF-1α* KO mice at P16 (See Supplementary Material and Supplementary Fig. S4, http://www.iovs.org/lookup/suppl/doi:10.1167/iovs.11-8936/-/DCSupplemental). In contrast, under hypoxic conditions, elevated levels of HIF-1α and VEGF were observed in the retinae from both the WT and *HIF-1α* KO mice, compared with those in WT mice under normoxic conditions. There was no significant difference in retinal levels of HIF-1α and VEGF between OIR WT mice and OIR *HIF-1α* KO mice (See Supplementary Material and Supplementary Fig. S5, http://www.iovs.org/lookup/suppl/doi:10.1167/iovs.11-8936/-/DCSupplemental).

Angiography with high molecular weight fluorescein–dextran demonstrated that both the WT and the conditional *HIF-1α* KO mice exhibited similar degrees of ischemia-induced retinal NV in the flat-mounted retina (See Supplementary Material and Supplementary Figs. S6A–D, http://www.iovs.org/lookup/suppl/doi:10.1167/iovs.11-8936/-/DCSupplemental). Quantification of pre-retinal neovascular cells further demonstrated that there was no significant difference in the number of preretinal nuclei between the OIR-treated conditional *HIF-1α* KO mice and OIR WT controls (See Supplementary Material and Supplementary Figs. S6E–G, http://www.iovs.org/lookup/suppl/doi:10.1167/iovs.11-8936/-/DCSupplemental). These results suggest that *HIF-1α* KO in the RPE does not attenuate ischemia-induced retinal NV.

Disruption of HIF-1α in the RPE Attenuates the Increase of HIF-1α and VEGF Protein Levels in Eyes with Laser-Induced CNV

To assess the role of RPE-derived HIF-1α in CNV, HIF-1α and VEGF protein levels in the eyecups with laser-induced CNV were measured by Western blot analysis 12 days after laser coagulation. HIF-1α and VEGF levels were significantly elevated in WT mice, while the increases were diminished in the conditional *HIF-1α* KO mice eyes (Figs. 3A–D). Immunohistochemistry further confirmed that interruption of *HIF-1α* in the RPE considerably attenuated VEGF overexpression in the laser lesions of conditional *HIF-1α* KO mice, compared with that of WT controls (Fig. 3E–G).

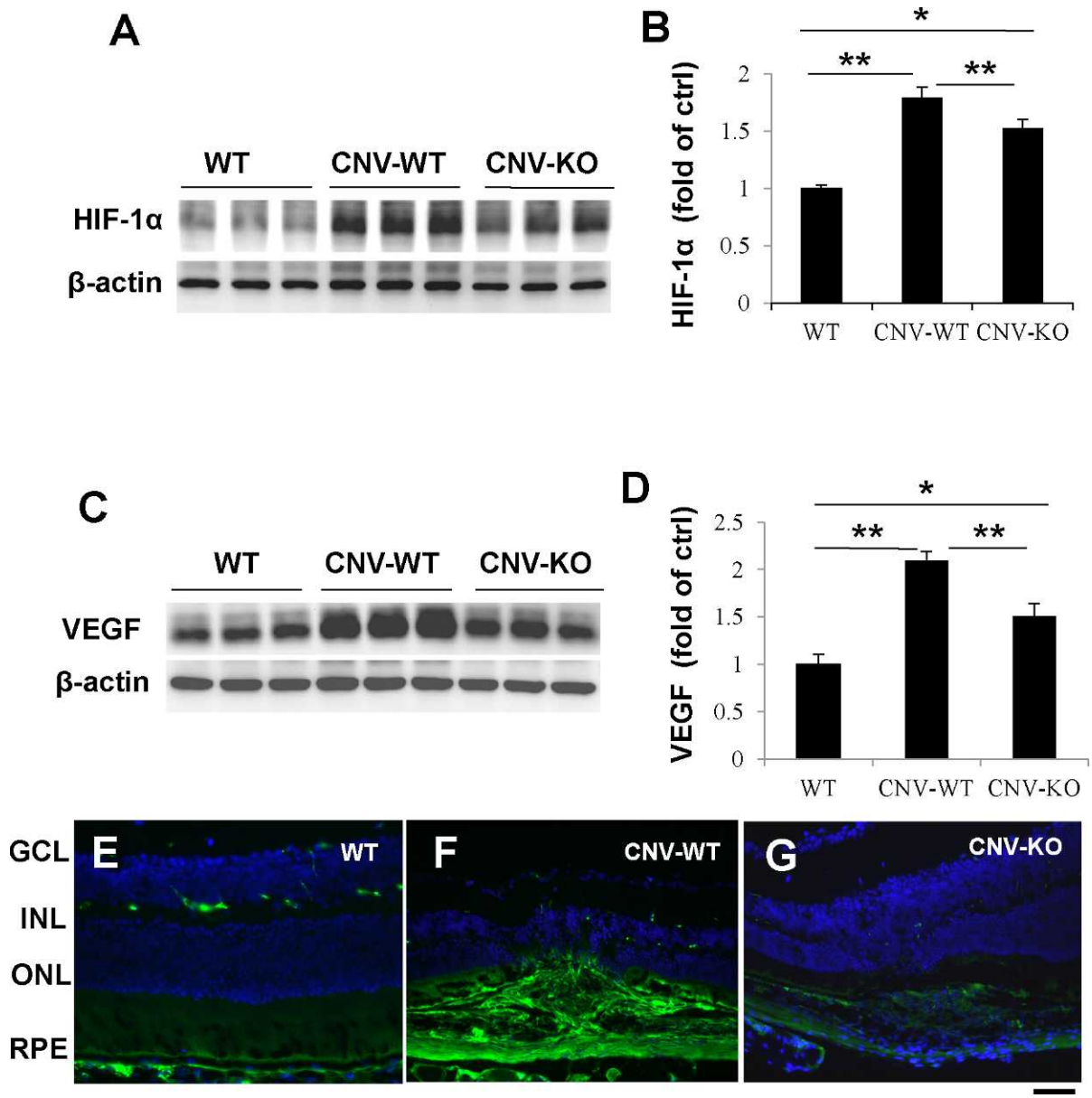

Figure 3. Attenuated increases of HIF-1α and VEGF levels in the eyecups from *HIF-1α* KO mice with laser-induced CNV. (**A, C**) Western blot analysis of HIF-1α (**A**) and VEGF (**C**) in the eyecups from WT mice and *HIF-1α* KO mice subjected to laser photocoagulation–induced CNV. (**B, D**) Densitometry analysis showed that increases of HIF-1α (**B**) and VEGF (**D**) were significantly attenuated in the *HIF-1α* KO mice with CNV, compared with the WT CNV mice (mean ± SEM, $n = 6$). $^{*}P < 0.05$; $^{**}P < 0.01$. (**E-H**) Immunohistochemistry showed that the intensity of VEGF staining (*brown*) was considerably lower in laser lesions in the *HIF-1α* KO mice, compared with that in the WT control. VEGF staining in WT mice with CNV (**E**); in *HIF-1α* KO mice with CNV (**F**); in WT mice without CNV (**G**). *Scale bar*, 50 μm.

Inflammation and Vascular Leakage Associated with Laser-Induced CNV are Ameliorated in the Eyes of HIF-1α KO mice

ICAM-1 is a major adhesion molecule and plays important roles in leukocyte adherence to the endothelium. Western blot analysis showed that ICAM-1 levels in the eyecups were similar in the WT and HIF-1α KO mice under normal conditions (Figs. 4A, 4B). In contrast, laser coagulation significantly up-regulated ICAM-1 expression in the WT mice (collected 12 days after laser coagulation); the induction of ICAM-1 was abolished in the conditional *HIF-1α* KO mice (Figs. 4C, 4D). Retinal vascular leakage was measured by extravascular albumin content in the perfused retina using Western blot analysis. Laser-induced CNV increased extravascular albumin levels in the retina of the WT mice, but not in the *HIF-1α* KO (Figs. 4C, 4D). Vascular leakage was also observed using fundus fluorescein angiography, which showed that the vascular leakage around the CNV area was alleviated in the conditional *HIF-1α* KO mice at different time points after the fluorescein injection, compared with that of the WT control (Figs. 4E–L).

Disruption of HIF-1α in the RPE Ameliorates Laser-Induced CNV

To evaluate the contribution of RPE-derived HIF-1α to CNV, angiography with high molecular weight fluorescein-dextran was performed 2 weeks after laser coagulation. The laser-

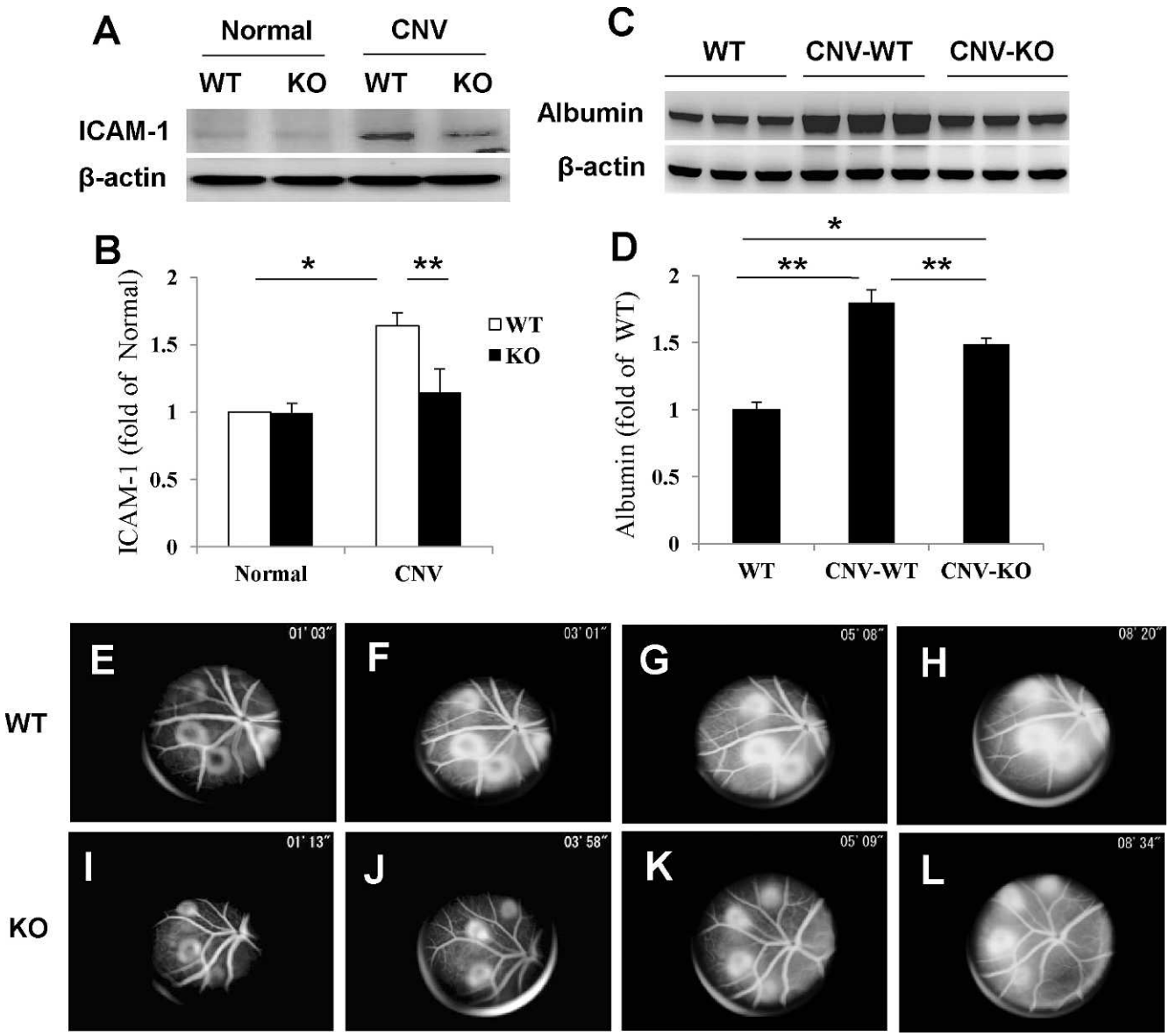

Figure 4. Comparison of ICAM-1 overexpression and vascular leakage in the eyes of the *HIF-1α* KO mice with laser-induced CNV. (**A, B**) ICAM-1 levels in eyecups with laser photocoagulation–induced CNV were measured by Western blot analysis and quantified by densitometry and normalized by β-actin levels (mean ± SEM, $n = 6$). (**C, D**) The retinae were dissected after thorough perfusion to remove blood in the vasculature. Serum albumin levels were then measured by Western blot analysis, quantified by densitometry and normalized by β-actin (mean ± SEM, $n = 6$). $^{*}P < 0.05$, $^{**}P < 0.01$. (**E–L**) Fluorescein angiography at different time points after the injection of fluorescein dextran showing lower vascular leakage around the CNV lesion in the *HIF-1α* KO mice (**I–L**), compared with that of WT control (**E–H**).

induced CNV was visualized by angiography in the flat-mounted RPE/choroid complex (Figs. 5A, 5B). The CNV area was measured using SPOT software and averaged. The results showed that CNV areas in the conditional *HIF-1α* KO mice were significantly smaller than that in WT controls (Fig. 5C).

Discussion

It is well known that the RPE has important physiological functions in the eye and is involved in some pathological conditions. The RPE is known to serve as the outer BRB and prevents macromolecules from entering the neural retina from the choroidal capillaries. In addition, the RPE and retinal Müller cells have been shown to produce high levels of pro-angiogenic and pro-inflammatory factors during ischemic conditions.[35,36] However, the contribution of RPE-derived pro-angiogenic factors and pro-inflammatory factors to ischemia-induced retinal inflammation and NV is not clear. Using a conditional gene KO mouse model, we have disrupted *HIF-1α* in the RPE. In the OIR model, the KO mice showed no difference from the WT mice in ischemia-induced retinal NV. In contrast, *HIF-1α* KO in the RPE attenuated laser-induced CNV and reduced vascular leakage from the neovasculature. These findings suggest that the RPE-derived HIF-1α plays a critical role in CNV, but not in ischemia-induced retinal NV.

To evaluate the post developmental function of HIF-1α in the RPE, we disrupted *HIF-1α* in the RPE using an inducible system at E15. Using this model, it was demonstrated that the loss of RPE cell-derived HIF-1α did not significantly reduce the expression of *VEGF* and other HIF-1α target genes or cause any

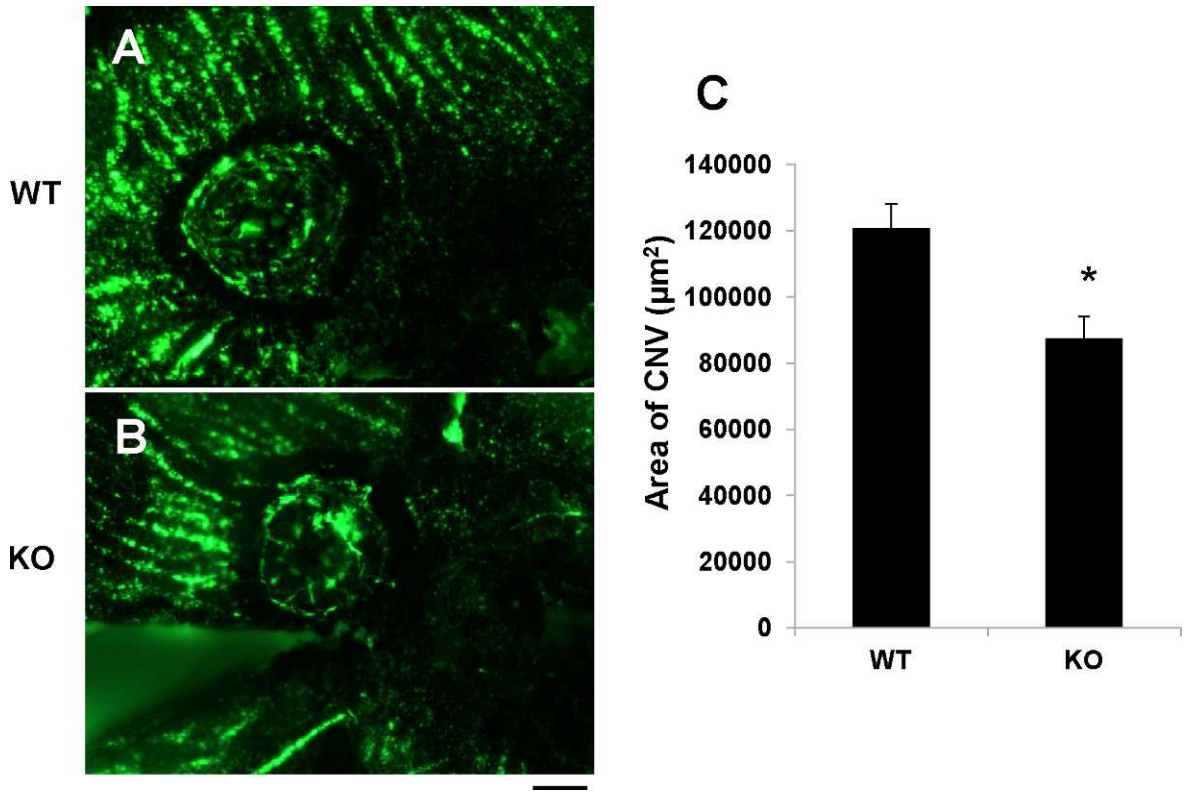

Figure 5. Amelioration of laser-induced CNV in the *HIF-1α* KO mice. (**A, B**) CNV was visualized by fluorescein angiography in flat-mounted RPE/choroid complex from the *HIF-1α* KO mice (**B**) and WT controls (**A**) 14 days after laser photocoagulation. *Scale bar*, 50 μm. (**C**) Quantification of the CNV area measured with SPOT software demonstrated decreased CNV area in the *HIF-1α* KO mice, compared with the WT control (mean ± SEM, $n = 5$). $^*P < 0.05$.

defects in retinal histological structure, retinal blood vessels or retinal function under normal conditions. These results suggest that postnatal *HIF-1α* KO in the RPE does not cause any developmental defects in the retina or retinal vasculature.

The possible explanations for the lack of a phenotype associated with ocular development in the *HIF-1α* KO mice under normal condition are: (1) in this study, the cultured primary RPE cells and the retina of the *HIF-1α* KO mice only showed an approximate 2-fold decrease in HIF-1α levels. It is likely that HIF-1α levels are in excess under normal conditions. The remaining HIF-1α in the RPE after the partial *HIF-1α* KO may be sufficient for retinal development, and (2) the target genes regulated by HIF-1α, such as *VEGF*, can also be activated by other transcription factors such as AP-1, SP-1, and Akt, which can compensate for the loss of HIF-1α function.[37]

Retinal inflammation is an important pathogenic feature of AMD.[3] Retina-derived HIF-1α has been suggested to play a role in retinal inflammation through the regulation of inflammatory factors such as VEGF.[35,38] Our results showed that *HIF-1α* KO in the RPE alone significantly attenuated overexpression of *VEGF* and *ICAM-1* in the CNV model, suggesting that RPE-derived HIF-1α plays an important role in retinal inflammation in the CNV model. Further, the *HIF-1α* KO also significantly alleviated albumin leakage into the retina in the CNV model. In the OIR model, however, *HIF-1α* KO in the RPE did not ameliorate the retinal inflammation or BRB breakdown induced by ischemia. These observations suggest that the RPE-derived HIF-1α plays an important role in the outer BRB breakdown, but not in the inner BRB breakdown.

Recent studies have illustrated that HIF-1α is the main sensor of ischemia, which plays a pivotal role in angiogenesis.[39] HIF-1α and VEGF levels are increased not only in experimental CNV models, but also in human CNV membranes, human retinal neovasculature and angiomatous specimens.[7,40–42] Anti-VEGF or anti–HIF-1α molecules have been shown to attenuate the formation of laser-induced CNV or ischemia-induced retinal NV.[43] CNV is the most common cause of visual impairment in the elderly with AMD.[44] Laser-induced CNV is a widely used model for wet AMD, since it develops CNV similar to that observed in AMD, in which the new vessels grow from the choroid and penetrate Bruch's membrane.[45] To study the role of RPE-derived HIF-1α in CNV, the *HIF-1α* KO mice were subjected to laser coagulation. These experiments showed that *HIF-1α* KO in RPE cells significantly reduced overexpression of *HIF-1α* and its targeted genes, reduced retinal inflammation and vascular leakage as well as attenuated laser-induced CNV. These observations suggest that the RPE-derived HIF-1α plays a key role in CNV. This finding not only provides new insights into the pathogenesis of CNV, but may also contribute to the development of cell-based therapeutics for AMD.

VEGF has been shown to play a key role in both laser-induced CNV and ischemia-induced retinal NV.[23,35] *VEGF* is regulated by multiple transcription factors in several pathways such as AP-1, SP-1, β-catenin, and Akt.[37] The specific role of HIF-1 in *VEGF* overexpression during CNV has not been defined. Using a conditional *HIF-1α* KO, the present study shows that HIF-1α in the RPE is responsible, at least in part, for the overexpression of *VEGF* in the CNV model. This observation is consistent with the recent study by Huang et al.[46] using prolyl hydroxylase-1 (PHD1)–deficient mice. PHD1-deficient mice showed decreased HIF-1α degradation and consequently, induced *VEGF* expression and reduced hyper-

oxia-induced vessel loss, suggesting a key role of HIF-1 in the regulation of *VEGF* expression.

It is well established that RPE cells produce high levels of VEGF and are the major source of VEGF in the laser-induced CNV model.[4,35] Further investigations have defined that there is a polarized secretion of VEGF by RPE cells in vitro and that up-regulated RPE basolateral VEGF secretion in hypoxia or loss of polarity of VEGF secretion may cause CNV.[20] In our study, the *HIF-1α* KO did not affect ischemia-induced retinal NV in the OIR model, suggesting that VEGF secreted into the retina has only a slight, if any, role in retinal NV.

Although our results demonstrated that RPE cell-derived HIF-1α is important for CNV, the results do not exclude the possibility that other retinal cells are also involved in this process. The outer BRB is responsible for approximately 80% of the oxygen supply in the eye.[47] A number of independent studies have demonstrated outer BRB breakdown in diabetes and ischemia.[48,49] Overexpression of *VEGF* has been shown to play a key pathogenic role in breakdown of the barrier and contributes to impaired tight-junction integrity in the outer BRB.[50] Recent studies indicate that *HIF-1α* may be regulated by multiple factors besides hypoxia, such as nitric oxide (NO), reactive oxygen species (ROS), Sirt1, nuclear factor kappa B[51]; HIF-2α, the isoform of HIF-1α, may be another important transcription factor up-regulated in CNV.[7] Further research with this conditional *HIF-1α* KO mice will facilitate clarifying the relationship between these signaling molecules and pathways.

In summary, the present study provides the first evidence showing that RPE cell-derived HIF-1α is a pivotal contributor to CNV. Targeting HIF-1α in RPE cells can potentially become a new therapeutic strategy for the treatment of AMD.

Acknowledgments

The authors thank Randal Johnson, PhD, at UCSD for providing the *HIF-1α*/floxed mice and Ira Blader, PhD, at the University of Oklahoma Health Sciences Center for assistance with the breeding of the *HIF-1α/floxP* mice.

References

1. Mechoulam H, Pierce EA. Retinopathy of prematurity: molecular pathology and therapeutic strategies. *Am J Pharmacogenomics*. 2003;3:261–277.
2. Rajappa M, Saxena P, Kaur J. Ocular angiogenesis: mechanisms and recent advances in therapy. *Ad Clin Chem*. 2010;50:103–121.
3. Campochiaro PA. Retinal and choroidal neovascularization. *J Cell Physiol*. 2000;184:301–310.
4. Kwak N, Okamoto N, Wood JM, Campochiaro PA. VEGF is major stimulator in model of choroidal neovascularization. *Invest Ophthalmol Vis Sci*. 2000;41:3158–3164.
5. Yang XM, Wang YS, Zhang J, et al. Role of PI3K/Akt and MEK/ERK in mediating hypoxia-induced expression of HIF-1alpha and VEGF in laser-induced rat choroidal neovascularization. *Invest Ophthalmol Vis Sci*. 2009;50:1873–1879.
6. Pouyssegur J, Dayan F, Mazure NM. Hypoxia signalling in cancer and approaches to enforce tumour regression. *Nature*. 2006;441:437–443.
7. Sheridan CM, Pate S, Hiscott P, Wong D, Pattwell DM, Kent D. Expression of hypoxia-inducible factor-1alpha and –2alpha in human choroidal neovascular membranes. *Graefes Arch Clin Exp Ophthalmol*. 2009;247:1361–1367.
8. Ke Q, Costa M. Hypoxia-inducible factor-1 (HIF-1). *Mol Pharmacol*. 2006;70:1469–1480.
9. Rey S, Semenza GL. Hypoxia-inducible factor-1-dependent mechanisms of vascularization and vascular remodelling. *Cardiovasc Res*. 2010;86:236–242.
10. Loboda A, Jozkowicz A, Dulak J. HIF-1 and HIF-2 transcription factors–similar but not identical. *Mol Cells*. 2010;29:435–442.
11. Wang GL, Jiang BH, Rue EA, Semenza GL. Hypoxia-inducible factor 1 is a basic-helix-loop-helix-PAS heterodimer regulated by cellular O2 tension. *Proc Natl Acad Sci U S A*. 1995;92:5510–5514.
12. Ivan M, Kondo K, Yang H, et al. HIFalpha targeted for VHL-mediated destruction by proline hydroxylation: implications for O2 sensing. *Science*. 2001;292:464–468.
13. Jaakkola P, Mole DR, Tian YM, et al. Targeting of HIF-alpha to the von Hippel-Lindau ubiquitylation complex by O2-regulated prolyl hydroxylation. *Science*. 2001;292:468–472.
14. Epstein AC, Gleadle JM, McNeill LA, et al. C. elegans EGL-9 and mammalian homologs define a family of dioxygenases that regulate HIF by prolyl hydroxylation. *Cell*. 2001;107:43–54.
15. Bruick RK, McKnight SL. A conserved family of prolyl-4-hydroxylases that modify HIF. *Science*. 2001;294:1337–1340.
16. Semenza GL. Hypoxia-inducible factor 1 (HIF-1) pathway. *Sci STKE*. 2007:cm8.
17. Saari JC. Biochemistry of visual pigment regeneration: the Friedenwald lecture. *Invest Ophthalmol Vis Sci*. 2000;41:337–348.
18. Zarbin MA. Current concepts in the pathogenesis of age-related macular degeneration. *Arch Ophthalmol*. 2004;122:598–614.
19. Thiersch M, Lange C, Joly S, et al. Retinal neuroprotection by hypoxic preconditioning is independent of hypoxia-inducible factor-1 alpha expression in photoreceptors. *Eur J Neurosci*. 2009;29:2291–2302.
20. Blaauwgeers HG, Holtkamp GM, Rutten H, et al. Polarized vascular endothelial growth factor secretion by human retinal pigment epithelium and localization of vascular endothelial growth factor receptors on the inner choriocapillaris. Evidence for a trophic paracrine relation. *Am J Pathol*. 1999;155:421–428.
21. Marneros AG, Fan J, Yokoyama Y, et al. Vascular endothelial growth factor expression in the retinal pigment epithelium is essential for choriocapillaris development and visual function. *Am J Pathol*. 2005;167:1451–1459.
22. Le YZ, Bai Y, Zhu M, Zheng L. Temporal requirement of RPE-derived VEGF in the development of choroidal vasculature. *J Neurochem*. 2010;112:1584–1592.
23. Witmer AN, Vrensen GF, Van Noorden CJ, Schlingemann RO. Vascular endothelial growth factors and angiogenesis in eye disease. *Prog Retin Eye Res*. 2003;22:1–29.
24. Bai Y, Ma JX, Guo J, et al. Müller cell-derived VEGF is a significant contributor to retinal neovascularization. *J Pathol*. 2009;219:446–454.
25. Tobe T, Ortega S, Luna JD, et al. Targeted disruption of the FGF2 gene does not prevent choroidal neovascularization in a murine model. *Am J Pathol*. 1998;153:1641–1646.
26. Catanuto P, Espinosa-Heidmann D, Pereira-Simon S, et al. Mouse retinal pigmented epithelial cell lines retain their phenotypic characteristics after transfection with human papilloma virus: a new tool to further the study of RPE biology. *Exp Eye Res*. 2009;88:99–105.
27. Chen Y, Hu Y, Moiseyev G, Zhou KK, Chen D, Ma JX. Photoreceptor degeneration and retinal inflammation induced by very low-density lipoprotein receptor deficiency. *Microvasc Res*. 2009;78:119–127.
28. Martin PM, Roon P, Van Ells TK, Ganapathy V, Smith SB. Death of retinal neurons in streptozotocin-induced diabetic mice. *Invest Ophthalmol Vis Sci*. 2004;45:3330–3336.

29. Park K, Chen Y, Hu Y, et al. Nanoparticle-mediated expression of an angiogenic inhibitor ameliorates ischemia-induced retinal neovascularization and diabetes-induced retinal vascular leakage. *Diabetes*. 2009;58:1902–1913.
30. Chen Y, Moiseyev G, Takahashi Y, Ma JX. RPE65 gene delivery restores isomerohydrolase activity and prevents early cone loss in Rpe65-/- mice. *Invest Ophthalmol Vis Sci*. 2006;47: 1177–1184.
31. Farjo KM, Moiseyev G, Takahashi Y, Crouch RK, Ma JX. The 11-cis-retinol dehydrogenase activity of RDH10 and its interaction with visual cycle proteins. *Invest Ophthalmol Vis Sci*. 2009; 50:5089–5097.
32. Zhang D, Kaufman PL, Gao G, Saunders RA, Ma JX. Intravitreal injection of plasminogen kringle 5, an endogenous angiogenic inhibitor, arrests retinal neovascularization in rats. *Diabetologia*. 2001;44:757–765.
33. Browning J, Wylie CK, Gole G. Quantification of oxygen-induced retinopathy in the mouse. *Invest Ophthalmol Vis Sci*. 1997;38:1168–1174.
34. Smith LE, Wesolowski E, McLellan A, et al. Oxygen-induced retinopathy in the mouse. *Invest Ophthalmol Vis Sci*. 1994;35: 101–111.
35. Adamis AP, Shima DT, Yeo KT, et al. Synthesis and secretion of vascular permeability factor/vascular endothelial growth factor by human retinal pigment epithelial cells. *Biochem Biophys Res Commun*. 1993;193:631–638.
36. Pierce EA, Avery RL, Foley ED, Aiello LP, Smith LE. Vascular endothelial growth factor/vascular permeability factor expression in a mouse model of retinal neovascularization. *Proc Natl Acad Sci U S A*. 1995;92:905–909.
37. Josko J, Mazurek M. Transcription factors having impact on vascular endothelial growth factor (VEGF) gene expression in angiogenesis. *Med Sci Monit*. 2004;10:RA89–98.
38. Arjamaa O, Nikinmaa M, Salminen A, Kaarniranta K. Regulatory role of HIF-1alpha in the pathogenesis of age-related macular degeneration (AMD). *Ageing Res Rev*. 2009;8:349–358.
39. Wenger RH, Gassmann M. Oxygen(es) and the hypoxia-inducible factor-1. *Biol Chem*. 1997;378:609–616.
40. Inoue Y, Yanagi Y, Matsuura K, Takahashi H, Tamaki Y, Araie M. Expression of hypoxia-inducible factor 1alpha and 2alpha in choroidal neovascular membranes associated with age-related macular degeneration. *Br J Ophthalmol*. 2007;91:1720–1721.
41. Ozaki H, Yu AY, Della N, et al. Hypoxia inducible factor-1alpha is increased in ischemic retina: temporal and spatial correlation with VEGF expression. *Invest Ophthalmol Vis Sci*. 1999; 40:182–189.
42. Shimada H, Kawamura A, Mori R, Yuzawa M. Clinicopathological findings of retinal angiomatous proliferation. *Graefes Arch Clin Exp Ophthalmol*. 2007;245:295–300.
43. Song SJ, Chung H, Yu HG. Inhibitory effect of YC-1, 3-(5′-hydroxymethyl-2′-furyl)-1-benzylindazole, on experimental choroidal neovascularization in rat. *Ophthalmic Res*. 2008; 40:35–40.
44. Bird A. Therapeutic targets in age-related macular disease. *J Clin Invest*. 2010;120:3033–3041.
45. Francois J, De Laey JJ, Cambie E, Hanssens M, Victoria-Troncoso V. Neovascularization after argon laser photocoagulation of macular lesions. *Am J Ophthalmol*. 1975;79:206–210.
46. Huang H, De Veire SV, Dala M, et al. Reduced retinal neovascularization, vascular permeability, and apoptosis in ischemic retinopathy in the absence of prolyl hydroxylase-1 due to the prevention of hyperoxia-induced vascular obliteration. *Invest Ophthalmol Vis Sci*. 2011;52:7565–7573.
47. Xu HZ, Le YZ. Significance of outer blood-retina barrier breakdown in diabetes and ischemia. *Invest Ophthalmol Vis Sci*. 2011;52:2160–2164.
48. Decanini A, Karunadharma PR, Nordgaard CL, Feng X, Olsen TW, Ferrington DA. Human retinal pigment epithelium proteome changes in early diabetes. *Diabetologia*. 2008;51: 1051–1061.
49. Wang J, Xu X, Elliott MH, Zhu M, Le YZ. Müller cell-derived VEGF is essential for diabetes-induced retinal inflammation and vascular leakage. *Diabetes*. 2010;59:2297–2305.
50. Ablonczy Z, Crosson CE. VEGF modulation of retinal pigment epithelium resistance. *Exp Eye Res*. 2007;85:762–771.
51. Majmundar AJ, Wong WJ, Simon MC. Hypoxia-inducible factors and the response to hypoxic stress. *Mol Cell*. 2010; 40:294–309.